Co-current and Counter-Current Operations for Steam Reforming of Heptane in a Novel CFB Membrane Reformer

Zhongxiang Chen *, and Said S.E.H. Elnashaie
Department of Chemical Engineering, Auburn University, Auburn, AL 36849, USA
*E-mail: chenzho@auburn.edu, Tel: 1-334-844-2051, Fax: 1-334-844-2063

ABSTRACT

Hydrogen production by steam reforming of higher hydrocarbon over nickel-supported catalyst is investigated in an earlier suggested novel Circulating Fast Fluidized Bed Membrane Reformer (**CFFBMR**). Palladium hydrogen membranes are used with co-current and counter-current operation modes. It is found that hydrogen production has a non-monotonic dependence upon the reaction temperature in the range of 623-823K. Between 623 and 723K, the yields of hydrogen decrease and then increase between 723 and 823K. This important phenomenon is investigated, discussed and explained. The simulation results shows that the reformer performance can be significantly improved using hydrogen membranes, especially in the counter-current operation mode. At low temperatures around 623K, both co-current and counter-current operation modes provide similar yields of hydrogen. While at temperature 723K and higher, the counter-current operation provides the highest yield of hydrogen.

Keywords: circulating fluidized bed, co-current, counter-current, hydrogen, membrane reformer, non-monotonic, steam reforming

INTRODUCTION

Steam reforming of hydrocarbons is the most important process for the production of hydrogen or synthesis gas [1-8]. Natural gas, mainly methane has been widely studied in different reactor configurations [5,9-17]. However,

the feedstock of steam reforming for hydrogen production varies from place to place because of the availability of hydrocarbons [2,18]. Recent years have shown progress in steam reforming technology resulting in cheaper plants and higher feedstock flexibility because of the better materials for reactors, better control of coking and better reforming catalysts [19,20]. Steam reforming of higher hydrocarbons is of great importance not only for hydrogen production as a fuel, but also in the chemical and petrochemical industries [1,4,18,21-23]. Industrial steam reformers are typically fixed beds made up of a large number of catalyst tubes, surrounded by a huge top or side fired furnace [24].

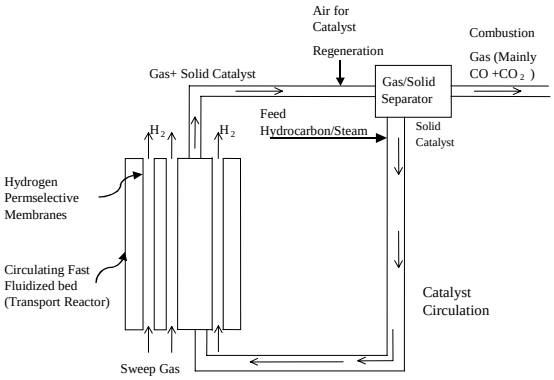

Fig. 1. Schematic of the circulating fast fluidized bed membrane reformer (**CFFBMR**)

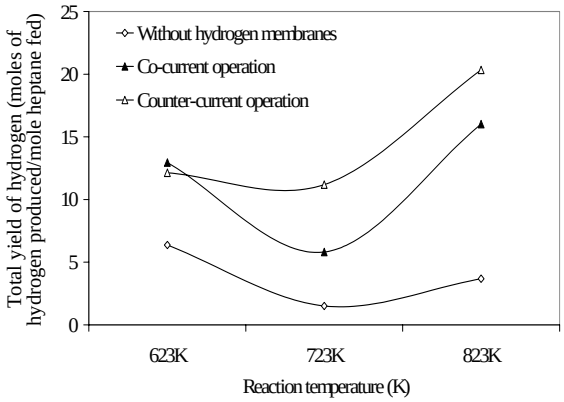

Fig.2. Non-monotonic behavior in hydrogen yield with respect to the reaction temperature in the **CFFBMR**

In this paper steam reforming of higher hydrocarbon heptane is investigated in a novel proposed Circulating Fast Fluidized Bed Membrane Reformer (**CFFBMR)**, which is shown in Fig.1. There are a number of palladium hydrogen membrane tubes where hydrogen permeates selectively from the reformer and then is carried away by sweep gas such as steam in the membrane tubes. The nickel reforming catalyst is fast fluidized and carried out of the reformer with the gas stream, regenerated along the exit line and separated in a gas-solid separator. The regenerated catalyst is recycled to the reformer. The continuous catalyst regeneration in the whole process makes the effect of carbon deposition on the catalyst activity negligible. An

interesting phenomenon that the hydrogen yield is non-monotonic with respect to the reaction temperature shown in Fig.2 is investigated.

REACTION KINETICS AND REFORMER MODELING

The following reaction scheme and kinetics are used to study steam reforming of heptane in the **CFFBMR** [1,3]:

$$C_7H_{16} + 7H_2O \rightarrow 7CO + 15H_2 \qquad r_1 = \frac{k_1 P_{C_7H_{16}}}{[1 + 25.2\frac{P_{C_7H_{16}} P_{H_2}}{P_{H_2O}} + 0.077\frac{P_{H_2O}}{P_{H_2}}]^2} \tag{1}$$

$$CO + 3H_2 = CH_4 + H_2O \qquad r_2 = k_2(\frac{P_{CH_4}P_{H_2O}}{P_{H_2}^{2.5}} - \frac{P_{CO}P_{H_2}^{0.5}}{K_2})/(1 + K_{CO}P_{CO} + K_{H_2}P_{H_2} + K_{CH_4}P_{CH_4} + K_{H_2O}P_{H_2O}/P_{H_2})^2 \tag{2}$$

$$CO + H_2O = CO_2 + H_2 \qquad r_3 = k_3(\frac{P_{CO}P_{H_2O}}{P_{H_2}} - \frac{P_{CO_2}}{K_3})/(1 + K_{CO}P_{CO} + K_{H_2}P_{H_2} + K_{CH_4}P_{CH_4} + K_{H_2O}P_{H_2O}/P_{H_2})^2 \tag{3}$$

$$CH_4 + 2H_2O = CO_2 + 4H_2 \qquad r_4 = k_4(\frac{P_{CH_4}P_{H_2O}^2}{P_{H_2}^{3.5}} - \frac{P_{CO_2}P_{H_2}^{0.5}}{K_2 \cdot K_3})/(1 + K_{CO}P_{CO} + K_{H_2}P_{H_2} + K_{CH_4}P_{CH_4} + K_{H_2O}P_{H_2O}/P_{H_2})^2 \tag{4}$$

A plug flow reactor model is used for reformer modeling. The model equations are summarized in Table 1. Co-current and counter-current operation modes with palladium hydrogen membranes are investigated.

Table 1. Model equations for isothermal **CFFBMR**

Reaction side	
Component i	$\frac{dF_i}{dl} = \rho_C(1-\varepsilon)\cdot A_f \cdot \sum_{j=1}^{J}\sigma_{i,j}r_j - a\cdot J_{H_2}\cdot\pi\cdot N_{H_2}\cdot d_{H_2}$ where a=0 for all components except for component hydrogen a=1
Boundary condition	at $l=0,\quad F_i = F_{i0}$
Hydrogen permeation side	
Hydrogen in membrane tubes	$\frac{dF_{H_2,P}}{dl} = b\cdot J_{H_2}\cdot\pi\cdot N_{H_2}\cdot d_{H_2}$ where b=1 for co-current operation and b=-1 for counter-current operation
Boundary condition	at $l=0,\quad F_{H_2,P} = F_{H_2,P0} = 0$ for co-current operation at $l=L,\quad F_{H_2,P} = F_{H_2,P0} = 0$ for counter-current operation
Hydrogen Permeation Flux	$J_{H_2} = \frac{Qe^{\frac{E_{H_2,P}}{RT}}}{\delta_{H_2}}(\sqrt{P_{H_2,r}} - \sqrt{P_{H_2,P}})$ [25]

RESULTS AND DISCUSSION

The main reformer construction parameters and simulation conditions are summarized in Table 2.

Table 2. Reformer construction parameters and reaction conditions for **CFFBMR**

CFBMR reformer construction parameters	
Length of the reformer and membrane tubes	2 m [24]
Diameter of the reformer tube	0.0978 m [24]
Diameter of palladium hydrogen membranes tubes	0.00489 m [24]
Thickness of palladium hydrogen membranes	20 μm [25]
Nickel steam reforming catalyst	
Catalyst particle density	2835 kg/m^3 [24]
Mean catalyst particle size	186 μm [13]
Solid fraction in circulating fast fluidization bed	0.2 [26]
Process gas feed rates and reaction conditions [1]	
Feed rate of heptane	0.178 mol/s
Feed rate of steam	2.5 mol/s
Steam to carbon ratio	2 mol/mol
Reaction temperature	623-823K
Reaction pressure	1013 kPa
Feed rate of sweep gas in hydrogen membrane tubes	0.278 mol/s
Operating pressure in palladium hydrogen membrane tubes	101.3 kPa

WITHOUT HYDROGEN SELECTIVE MEMBRANES

First the isothermal **CFFBMR** is studied at 623, 723 and 823K for the cases without any palladium hydrogen membranes. The lowest curve in Fig.2 shows that the yield of hydrogen for this case is non-monotonic with respect to the reaction temperature. At 623K the yield of hydrogen is 6.37 moles of hydrogen per mole of heptane fed. While at 723K it is 1.50 and 3.68 at 823K. Fig.3 shows that at low temperature 623K, the conversion of heptane increases along the reactor length but heptane is not fully converted before exiting the **CFFBMR**. While at higher temperatures 723 and 823K, heptane is

fully converted and the reactor length for heptane full conversion is about 0.3m at 823K and 0.8m at 723K. Further investigation shows that thermodynamic equilibrium state is established after the full conversion of heptane in the reformer due to the fast reversible methanation, water gas shift and steam reforming of methane, resulting in a constant flow rate of methane along the rest reactor length in Fig.4, similar to the other components in the reformer.

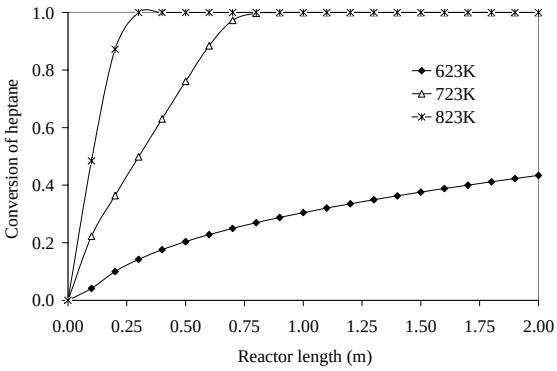

Fig.3. Conversion of heptane at 623, 723 and 823K without any palladium hydrogen membranes for isothermal **CFBMR** simulation

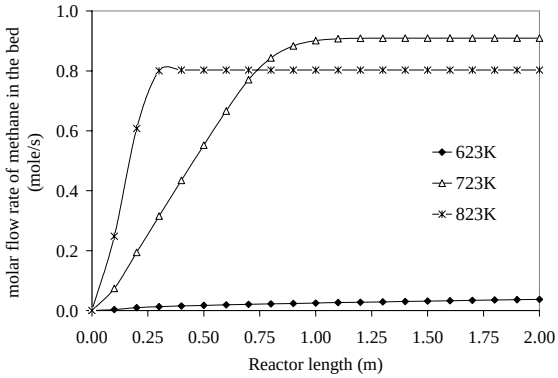

Fig.4. Molar flow rate of methane at 623, 723 and 823K without any palladium hydrogen membranes for isothermal **CFBMR** simulation

Table 3(a) shows the exit dry product gas composition (excluding steam) in the **CFFBMR**. At 623K heptane is not fully converted. The main products are hydrogen (64.42mol%), carbon monoxide (23.06mol%) and carbon dioxide (4.85mol%). The product distribution shows that heptane steam reforming (reaction 1) is the dominant reaction in the system at 623K and the second important reaction is water gas shift (reaction 3). While the methanation reaction (2) is not important at this low temperature. Since hydrogen is continuously produced by steam reforming of heptane, thermodynamic equilibrium can not establish among the reversible methanation, steam reforming of methane and water gas shift reactions. However, at 723K heptane is fully converted (Fig.3) and then the thermodynamic equilibrium

state is established, resulting in a constant flow rate of methane (Fig.4). The main products at 723K are methane (59.14mol%), carbon dioxide (21.33mol%) and hydrogen (19.09mol%). Thus at 723K the methanation (reaction 2) is dominant, which leads to a very high composition of methane. Because 3 moles of hydrogen is consumed to produce 1 mole of methane by the methanation reaction (2), the higher the gas composition of methane, the lower the gas composition of hydrogen and the lower the yield of hydrogen. At 723K the gas composition of carbon dioxide is as high as 21.33mol%, which shows that the water gas shift (reaction 3) is favored for hydrogen production. However, the improvement of hydrogen production by water gas shift is relatively small to address the significant consumption of hydrogen by methanation. As a result the overall yield of hydrogen at 723K is very low (Fig.2). At 823K the methantion reaction still dominates the reforming system with 41.67mol% of methane. The water gas shift reaction is also favored for hydrogen production with 20.62mol% of carbon dioxide. Compared to the case at 723K, the gas composition of methane is about 18mol% lower, and therefore steam reforming of methane becomes more and more important at 823K, which favors hydrogen production. Because the methantion reaction is still significant at 823K, the yield of hydrogen is lower than that at 623K. The non-monotonic behavior of hydrogen yield with respect to the reaction temperature is due to the importance of these competitive reactions that consume and/or produce hydrogen.

Table 3. Dry product gas composition (mol%)

	a): Without hydrogen membranes			b): Co-current operation			c): Counter-current operation		
	623 K	723 K	823 K	623 K	723 K	823 K	623 K	723 K	823 K
C_7H_{16}	5.59	0.0	0.0	0.85	0	0	0.89	0	0
CH_4	2.08	59.14	41.67	0.61	31.13	5.98	0.65	0.81	0.57
CO	23.06	0.44	2.29	26.08	0.42	1.89	29.26	0.04	1.34
CO_2	4.85	21.33	20.62	3.93	22.46	22.34	2.12	37.86	23.55
H_2	64.42	19.09	35.42	68.52	45.99	69.79	67.08	61.30	74.54

The reported hydrogen yield from steam reforming of heptane in a fixed bed reformer is about 2.0 at 723K and 1489kPa [27]. While the simulated hydrogen yield in the **CFFBMR** is about 2.4, which is the equilibrium hydrogen yield. Both the experimental and simulation results show that the steam reforming system suffers from the thermodynamic equilibrium limitation for hydrogen production due to the reversible reactions, especially the methanation reaction for steam reforming of higher hydrocarbons.

WITH PALLADIUM HYDROGEN SELECTIVE MEMBRANES

CO-CURRENT OPERATION

As mentioned above, the hydrogen production from steam reforming of heptane suffers from the thermodynamic equilibrium limitation. It can be "broken" using hydrogen selective membranes. The removal of hydrogen will decrease the partial pressure of hydrogen, shifting the reactions to the direction for hydrogen production. Table 3(b) shows the exit dry product gas composition for the case with hydrogen membranes under co-current operations. The trend of the product composition is similar to the case without hydrogen membranes except for the fact that much lower composition of methane and much higher composition of hydrogen are achieved at 723 and 823K. As discussed earlier, at 623K steam reforming of heptane is dominant in the system and no thermodynamic equilibrium is developed because heptane is not fully converted. The methanation reaction is also not so significant as that at higher temperatures. The composition of methane at 623K is 0.61mol%. However, the compositions of methane at 723 and 823K are 31.13mol% and 5.98mol%, respectively, which are much lower than the case without hydrogen selective membranes in Table 3(a). Thus the composition of methane in the products is reduced by 47.36% for 723K and 85.65% for 823K due to the use of hydrogen selective membranes. Obviously,

the removal of hydrogen suppresses the formation of methane or enhances the steam reforming of methane. As a result, the composition of methane decreases. However, Table 3(b) also shows that at 723K the methanation reaction is still significant. Using hydrogen selective membranes, the removal of hydrogen decreases the concentration of hydrogen and also shifts the reversible water gas shift to the direction of hydrogen production, making the composition of carbon dioxide higher. Therefore the hydrogen yield is higher than the case without hydrogen membranes. For example, under co-current operation the hydrogen yield is 12.95 at 623K, 5.81 at 723K and 16.02 at 823K, respectively. Compared with the cases without hydrogen selective membranes, it is increased by 103.3%, 287.3% and 335.3%, respectively. Undoubtedly the **CFFBMR** performance is improved significantly using hydrogen selective membranes.

Although the hydrogen yield is significantly improved under co-current operation, it is still non-monotonic in relation to the reaction temperature as shown in Fig.2. The hydrogen yield at 723K is much lower than that at 623 and 823K. Further investigation shows that at 723K the dominant methanation reaction takes place continuously. As a result the flow rate of methane keeps increasing along the reformer length, which consumes a lot of hydrogen. On the other hand, heptane is fully converted at the reactor length about 0.5m in the reformer. Then after the reactor length of 0.5m the main contribution of hydrogen production by heptane stops, making the net hydrogen production rate negative along the rest of the reformer length. Since 3 moles of hydrogen are consumed for 1 mole of methane formation, the consumption of hydrogen is so fast that the partial pressure of hydrogen in the reaction side decreases steeply as shown in Fig.5. This steep drop makes the partial pressure of hydrogen in the reaction side lower than that in the membrane side. And therefore back permeation of hydrogen occurs and leads to a much lower yield of hydrogen at 723K. At 823K, although heptane is also

fully converted (at the reactor length 0.25 m), the partial pressure of hydrogen in the reaction side is not lower than that in the hydrogen membrane side because steam reforming of methane is becoming more and more important at 823K. As a result the production of methane is suppressed and more hydrogen is produced (see Table 3(b)). The hydrogen produced from the steam reforming of methane (or the suppression of methanation) in the reaction side addresses the steep drop of the partial pressure of hydrogen, making the system better for the continuous removal of hydrogen (Fig.6). Thus at 823K there is no back permeation of hydrogen found in the simulation. For the problem of back permeation at 723K, one may get rid of it by increasing the sweep gas flow rate in hydrogen membranes or using counter-current operations. In this work the velocity of the sweep gas in the hydrogen membranes is already high and we keep it constant to meet the limitation for industrial practice and application.

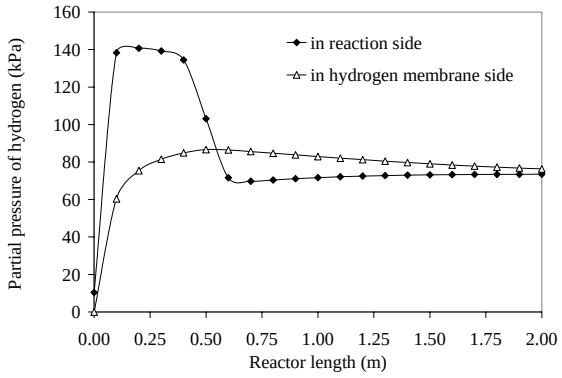

Fig.5. Partial pressures of hydrogen in the reaction side and hydrogen membrane side at 723K under co-current isothermal simulation

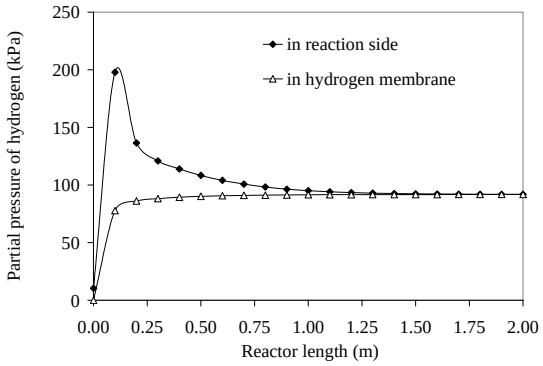

Fig.6. Partial pressures of hydrogen in the reaction side and hydrogen membrane side at 823K under co-current isothermal simulation

COUNTER-CURRENT OPERATION

In Table 1 the counter-current operation can be described as a two-point boundary value problem since the hydrogen exit flow is at the entrance of the

reformer. In this paper this problem is solved as a one-dimension searching problem. One general optimization technique, Flexible Tolerance Optimization Method (**FTOM**) is used to solve this problem [28]: Giving an initial guess of hydrogen flow rate at the exit of hydrogen membrane tubes (where is also the inlet of the reformer), then using the **CFFBMR** model to simulate the counter-current operations. At the exit of the reformer (or the entrance of the hydrogen membrane tubes), the simulated hydrogen flow rate in hydrogen membranes is compared to the initial entrance flow rate of hydrogen in the membranes, which is zero in this paper. If the simulated hydrogen flow rate is not zero, then use the **FTOM** to optimize the searching direction and step size to find the solution. If the initial or the new searching guesses for hydrogen exit flow rate in the membrane side is too small, then the solution obtained from the optimization could be the "false" or non-physical meaning solution. This kind of solution is usually called "trick" or "false" solution. In order to avoid this kind of "trick" solutions, Fig.7 is used to help to find the final right solution, which is plotted based on a series of searching data. For every initial guess of hydrogen exit flow rate, another flow rate of hydrogen at the entrance of the membrane can be obtained. Then the interception on the x-axis is the right solution, otherwise the simulated "solutions" on the left side of this interception are "trick" or "false" solutions.

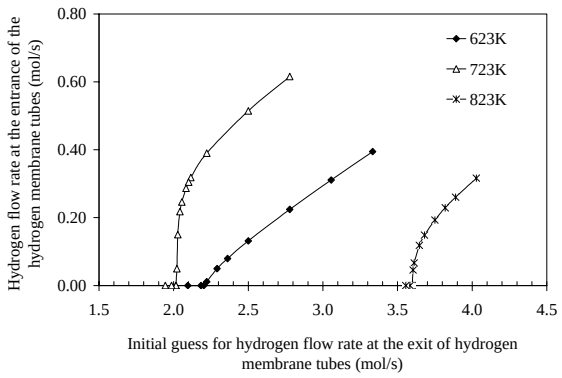

Fig.7. One-dimension searching for hydrogen exit flow rate in the membrane tubes under counter-current isothermal simulation

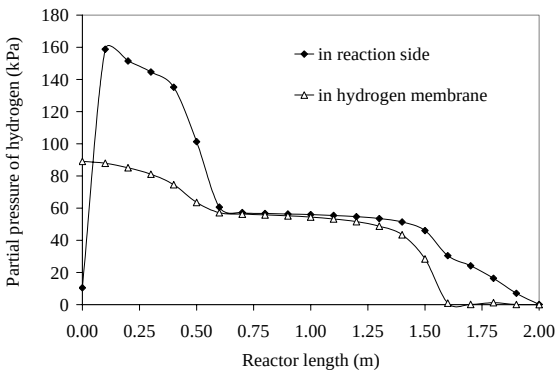

Fig.8. Partial pressures of hydrogen in the reaction side and hydrogen membrane side at 723K under counter-current isothermal simulation

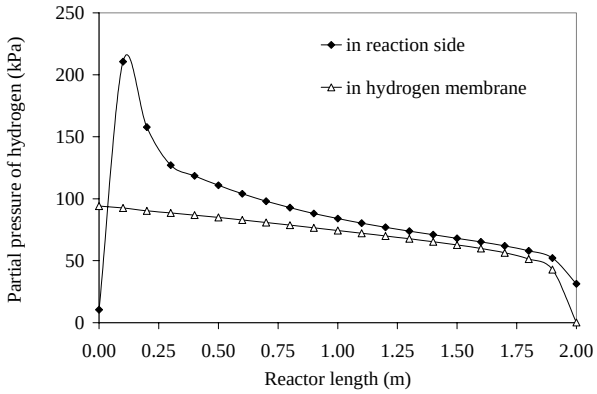

Fig.9. Partial pressures of hydrogen in the reaction side and hydrogen membrane side at 823K under isothermal counter-current simulation

With the right solution for the two-point boundary value problem under counter-current operation, the yields of hydrogen are obtained as shown in Fig.2. Table 3(c) shows the exit dry product gas composition. The main differences between counter-current and co-current operations are: (1) the composition of methane under counter-current operation at 723K is 0.81mol%, while it is 31.13mol% under co-current operation; (2) the composition of carbon dioxide under counter-current operation at 723K is 37.86mol%; while it is 22.46mol% under co-current operations. The compositions of other components are almost the same for both operation modes. Thus the yield of hydrogen at 723K is much higher than the case without hydrogen membranes and also higher than the case with hydrogen membranes under co-current operation mode. The reason for this improvement can be explained by the difference in the driving force for the hydrogen permeation. As shown in Figs.5 and 6, there is very small or even negative differential partial pressure of hydrogen under co-current operation after heptane full conversion, the performance of hydrogen membranes becomes inefficient or worse (for example, back permeation at 723K). However, under counter-current operation the differential partial pressures of hydrogen between the reaction side and the hydrogen membrane sides are

larger, as shown in Figs.8 and 9 for 723 and 823K. Therefore under counter-current operation more hydrogen is removed and higher hydrogen yields are obtained for both temperatures at 723 and 823K.

REFERENCES

1. Tottrup, P.B., Evaluation of Intrinsic Steam Reforming Kinetic Parameters from Rate Measurments on Full Particle Size, *Applied Catalysis*, 4 1982, p377-389.
2. Twigg M. V., *Catalyst Handbook*, 2nd Edition, Wolfe Publishing Ltd, 1989.
3. Xu, J., G.F. Froment, Methane Steam Reforming, Methanation and Water-Gas Shift: I. Intrinsic Kinetics, *J. AIChE*, 35 (1), 1989, p88-96.
4. Christensen, T. S., Adiabatic Prereforming of Hydrocarbons – an Important Step in Syngas Production, *Applied Catalysis A: General*, 138, 1996, p285-309.
5. Adris, A. M., Lim, C.J. and Grace, J.R., "The Fluidized-bed Membrane Reactor for Steam Methane Reforming: Model Verification and Parametric Study", *Chem. Eng. Sci*., 52, p1609-1622, 1997.
6. Ding, Y., E.Alpay, Adsorption-enhanced Steam-Methane Reforming, *Chem. Eng. Sci.*, 55,2000, p3929-3940.
7. Froment, G.F., Production of synthesis gas by steam- and CO_2-reforming of natural gas, *Journal of Molecular catalysis A: Chemical* 163, 2000, P147-156.
8. Hou, K., M.Fowles and R. Hughes, The Effect of Hydrogen Removal during Methane Steam Reforming in Membrane Reactors in the Presence of Hydrogen Sulphide, *Catalysis Today*, 56, 2000, p13-20.

9. Elnashaie S.S.E.H and Adris, A., “Fluidized Bed Steam Reformer for Methane”, *Proceedings of the IV International Fluidization Conference*, Banff, Canada, May 1989.
10. Adris, A., Elnashaie, S.S.E.H., and Hughes, R., “Fluidized Bed Membrane Steam Reforming of Methane”, *Can. J. Chem. Eng*., vol. 69, p1061 – 1070, 1991.
11. Hayakawa T., A.G. Andersen, M. Shimizu, K. Suzuki and K. Takehira, “Partial oxidation of methane to synthesis gas over some Tibanates based Perovskite oxides”, *Catal. Lett*., 22, p307-317, 1993.
12. Adris, A., Grace, J., Lim, C. and Elnashaie, S.S.E.H**.,** “Fluidized Bed Reaction System for Steam/ Hydrocarbon Gas Reforming to Produce Hydrogen", *US Patent no 5,326,550*, Date: June 1994a.
13. Adris, A. M., Lim, C.J. and Grace, J.R., “The Fluidized Bed Membrane Reactor (FBMR) System: a Pilot Scale Experimental Study”, *Chem. Eng. Sci*., 49, p5833-5843, 1994b.
14. Dyer,P.N.and Chen, C.M., “Engineering Development of Ceramic Membrane Reactor System for Converting Natural Gas to H_2 and Syngas for Liquid Transportation Fuel”, *Proceedings of the 1999 Hydrogen Program Review*, DOE, 1999.
15. Makel, D., “Low Cost Microchannel Reformer for Hydrogen Production from Natural Gas”, California Energy Commission (CEG), *Energy Innovations Small Grant (EISG) Program*, 1999.
16. Dyer, P.N. and Chen, C.M., “Engineering Development of Ceramic Membrane Reactor System for Converting Natural Gas to H_2 and Syngas for Liquid Transportation Fuel”, *Proceedings of the 2000 Hydrogen Program Review*, DOE, 2000.
17. Sammels, A. F., Schwartz, M., Mackay, R.A., Barton, T.F., and Peterson, D.R., “Catalytic Membrane Reactors for Spontaneous Synthesis Gas Production”, *Catalysis Today*, 56, p325, 2000.

18. Rostrup-Nielsen, J., Hydrogen via Steam Reforming of Naphtha, *Chem. Eng. Prog.*, 9, 1977, p87-92.
19. Rostrup-Nielsen J., J.H. Bak Hansen, L.U. Apricio, *J. Jpn. Petr. Inst*., 40, 1997, p366.
20. Rostrup-Nielsen J., I. Dybkjaer, in: *Proceedings of the First European Congress on Chemical Engineering*, Vol. 1, Firenze, May 4-7, 1997, p327.
21. Phillips, T.R., J.Mulhall and G.F.Turner, The Kinetics and Mechanism of the Reaction between Steam and Hydrocarbons over Nickel Catalysts in the Temperature Range 350-500^{o}C, Part I, *J. Catal*., 15, 1969, p233-244.
22. Bhatta, K.S.M.,and G.M. Dixon, Role of Urania and Alumina as Supports in the Steam Reforming of n-Butane at Pressure over Nickel-containing Catalysts, *Ind. Eng. Chem. Prod. Res. Develop*, 8, 1969, p324-331.
23. Rostrup-Nielsen, J.R., Activity of Nickel Catalysts for Steam Reforming of Hydrocarbons, *J. Catal*., 31, 1973, p173-199.
24. Elnashaie, S.S.E.H.; Elshishini, S.S., *Modelling, Simulation and Optimization of Industrial Fixed Bed Catalytic Reactors*, Gordon and Breach Science Publishers: London, 1993.
25. Shu, J., B.P.A. Grandjean and S. Kaliaguine, Methane Steam Reforming in asymmetric Pd- and Pd-Ag/porous SS Membrane Reactor, *Appl. Catal*, A 119, 1994, p305-325.
26. Kunii, D; Levenspiel, O., Circulating Fluidized-bed Reactors, *Chem. Eng. Sci.*, **1997**, 52(15), p2471-2482.
27. Phillips, T.R., J.Mulhall and G.F.Turner, The Kinetics and Mechanism of the Reaction between Steam and Hydrocarbons over Nickel Catalysts in the Temperature Range 350-500^{o}C, Part II, *J. Catal*., 17, 1970, p28-34.

28. Himmelblau D.M., Applied Nonlinear Programming, McGraw-Hill Book Company, N.Y., 341(1972).